OPEN

PRS GLOBAL OPEN

ORIGINAL ARTICLE
Research

Combined Face and Whole Eye Transplantation: Cadaveric Rehearsals and Feasibility Assessment

Hilliard T. Brydges, BS*
Ogechukwu C. Onuh, BA*
Bachar F. Chaya, MD*
David L. Tran, MD*
Michael F. Cassidy, BA*
Vaidehi S. Dedania, MD†
Daniel J. Ceradini, MD*
Eduardo D. Rodriguez, MD, DDS*

Background: In properly selected patients, combined face and whole eye transplantation (FWET) may offer a more optimal aesthetic and potentially functional outcome while avoiding the complications and stigma of enucleation and prosthetics. This study presents the most comprehensive cadaveric assessment for FWET to date, including rehearsal allograft procurement on a brain-dead donor.
Methods: Over a 2-year period, 15 rehearsal dissections were performed on 21 cadavers and one brain-dead donor. After identification of a potential recipient, rehearsals assessed clinical feasibility and enabled operative planning, technical practice, refinement of personalized equipment, and improved communication among team members. Operative techniques are described.
Results: Facial allograft procurement closely followed previously described face transplant techniques. Ophthalmic to superficial temporal (O-ST) vessel anastomosis for globe survival was assessed. Craniectomy allowed for maximal optic nerve and ophthalmic vessel pedicle length. Appropriate pedicle length and vessel caliber for O-ST anastomosis was seen. Research procurement demonstrated collateral blood flow to the orbit and surrounding structures from the external carotid system as well as confirmed the feasibility of timely O-ST anastomosis. Personalized cutting guides enabled highly accurate bony inset.
Conclusions: This study formalizes an approach to FWET, which is feasible for clinical translation in judiciously selected patients. O-ST anastomosis seems to minimize retinal ischemia time and allow perfusion of the combined allograft on a single external carotid pedicle. Although restoration of vision likely remains out of reach, globe survival is possible. *(Plast Reconstr Surg Glob Open 2023; 11:e5409; doi: 10.1097/GOX.0000000000005409; Published online 16 November 2023.)*

INTRODUCTION

The primary indication for face transplantation (FT) is restoration of the functional structures of the central face, which remain poorly reparable through traditional autologous methods.[1] Over the nearly 20-year history, of FT, surgeons have successfully transplanted a variety of structures, including the nose and nasal mucosa, lips and dentition, ears, neck, scalp, pharynx, and larynx.[2] FT has also proven valuable for the restoration of the eyelids, the function of which is integral to the maintenance of a healthy globe and limiting vision-related complications.[3] However, for patients whose defects include enucleation, transplantation of the eyelids without underlying globe support may lead to suboptimal aesthetic and periorbital functional outcomes.[4,5] Although orbital prosthetics may reduce the risk of these adverse events, they are suboptimal aesthetically, require considerable upkeep, and increase the risk of many adverse events, including ulcers, infections, and tissue retraction.[6,7] Although suboptimal in all patients, infection risks are exacerbated in immunosuppressed FT patients, whereas both infection and ulceration may be inciting events for transplant rejection.[8] For this reason, recent literature has explored the potential of whole eye transplantation in the setting of FT.[9] Irrespective of the potential for vision restoration, in properly selected patients, combined face and whole eye transplantation (FWET) may offer

*From *Hansjorg Wyss Department of Plastic Surgery at NYU Grossman School of Medicine, New York, N.Y; and †Department of Ophthalmology at NYU Grossman School of Medicine, New York, N.Y.*

Received for publication August 28, 2023; accepted September 26, 2023.

DOI: 10.1097/GOX.0000000000005409

Disclosure statements are at the end of this article, following the correspondence information.

Related Digital Media are available in the full-text version of the article on www.PRSGlobalOpen.com.

a more optimal aesthetic and potentially functional outcome, while avoiding the complications of enucleation and orbital prosthetics.

Over its near 20-year history, the field of FT has achieved many notable milestones.[10–12] Its success, like all reconstructive surgery, finds its foundation in the mastery of clinical anatomy, with particular emphasis on the principles of craniofacial surgery and microsurgery. Cadaveric studies offer a high-fidelity simulation in preparation for these exceptionally personalized procedures, giving clinicians an opportunity to define a technical approach, refine surgical skills, develop custom equipment, and improve teamwork and coordination. FT rehearsals have been seen to improve operative timing and precision and, by implication, patient outcomes.[10,13,14] In this study, we describe our experience with cadaveric rehearsals for a FWET, including the first research procurement (RP) in a brain-dead donor. All rehearsals were conducted after identification of a potential recipient; thus, technical and logistical considerations necessary for clinical translation are described.

Takeaways

Question: Would it be technically feasible to perform a combined face and whole eye transplantation? Could this be replicated in a cadaveric study?

Findings: Fifteen rehearsal dissections over the span of 2 years demonstrate that facial allograft procurement designed to include an orbit can be feasibly performed with the inclusion of a superficial temporal artery to ophthalmic artery bypass, allowing for orbital perfusion solely through the external carotid.

Meaning: Clinical translation of a facial allograft that includes an orbital component is possible by designing primary perfusion of the combined allograft on a single external carotid pedicle.

MATERIALS AND METHODS

Rehearsal Progression

Over a nearly 2-year period from August 2021 to March 2023, 15 rehearsal dissections involving 21 cadavers and one brain-dead donor were performed. Broadly, rehearsals were grouped into four categories: three cadaveric rehearsal types and one RP. A detailed breakdown of rehearsal types, goals, staff involved, and materials used can be found in Table 1. All cadavers were screened for infectious diseases but were selected without any prescreening for demographic, cephalometric, or clinical characteristics. This was done intentionally to allow for the randomization of anthropometric attributes as well as to promote the maximal clinical challenge with the goal of preemptive identification of potential operative issues. A subset of cadavers were treated with silicon vascular injections for improved identification and discernment of arterial and venous vasculature. This article and the rehearsals described conform to the Declaration of Helsinki.

Table 1. Overview of Rehearsals, Including Number of Rehearsals, Donor Tissue Evaluated, Location of Rehearsal, Staff Involved, Material Used, and Goals

Rehearsal Type	Rehearsal Count	Donor Tissue Count	Donor Tissue Assessed	Location, Staff and Material	Goal
Procurement design	7	Per rehearsal : 1 (donor) Total: 7	Silicon injected	Cadaver laboratory. No specialized equipment. Procurement team surgeons only.	Indentify approach to orbit, preserving maximal optic nerve length, while limiting both risks to the ophthalmic vessels and retinal ischemia time. High-level design of donor cutting guides.
Recipient and inset design	4	Per rehearsal : 2 (1 donor, 1 recipient) Total: 8	1 Silicon injected and 1 untreated	Cadaver laboratory. No specialized equipment. Procurement and donor preparation team surgeons only. Postoperative CT scan (beginning with second rehearsal)	After identification of a potential donor, aimed to practice the donor preparation. Design recipient cutting guides. Refine recipient cutting guides. Practice allograft inset.
Operative rehearsals	3	Per rehearsal : 2 (1 donor, 1 recipient) Total: 6	1 Silicon injected and 1 untreated	Operating room. Operating room surgical eqiupment. Procurement and donor preparation team surgeons, operating room staff, including scrub techs and nurses. Postoperative CT scan.	All of the above. In addition, preparation of OR staff. Team dynamics rehearsal. Identification of potential issues and needs for specialized equipment
Research procurement	1	Per rehearsal : 1 (donor) Total: 1	Brain-dead donor	Operating room. Operating room surgical eqiupment. Procurement team surgeons, operating room staff, including scrub techs, nurses, and anesthesiologists.	All of the above. In addition, highest fidelity technical practice, including hemostasis. Identification of real-world constraints and challenges. Assess microvascular considerations.
Total	15	Total: 22	14 silicon injected 7 untreated 1 brain-dead donor	11 Cadaver laboratory 4 Operating room	

Printed with permission and copyrights retained by Eduardo D. Rodriguez, MD, DDS.

Research Procurement

RP was conducted on a brain-dead donor, with the informed consent of the family. Following identification, the donor was transferred to the preoperative area, where they were evaluated by the anesthesia team, and both pupils were dilated with 1% tropicamide and 2.5% phenylephrine HCl.

After transfer to the operating room (OR), the patient underwent bilateral ocular evaluation by a retinal ophthalmologist with expertise in vitreoretinal disease. Fundic photography using RETCam and optical coherence tomography demonstrated bilateral wet macular degeneration. A tracheostomy was then performed, and the procurement began. [**See figure, Supplemental Digital Content 1,** which shows a color fundus photograph (without fluorescein angiography) (top) demonstrating macular subretinal scarring (yellow arrow) and peripheral subretinal hemorrhage (green arrowhead). **http://links.lww.com/PRSGO/C864**.] [**See figure, Supplemental Digital Content 2**, which shows that the optical coherence tomography B-scan (cross-section, middle) demonstrated retinal elevation consistent with subretinal fibrosis (red arrow) secondary to age-related macular degeneration, with retinal pigment epithelium reference line (yellow arrows). **http://links.lww.com/PRSGO/C865**.] [**See figure, Supplemental Digital Content 3**, which shows an optical coherence tomography en face image consistent with wet age-related macular degeneration (bottom). **http://links.lww.com/PRSGO/C866**.]

Procurement Approach: Skin and Soft Tissue

Skin and soft tissue markings were performed (Fig. 1). Bilateral incisions started on the neck lateral to the clavicular attachment of the sternocleidomastoid, proceeding superiorly on the lateral neck posterior to the angle of the mandible, then preauricular along the face. At the level of the right zygomatic arch, incisions tracked medially along the superior zygomatic body, to the lateral canthus before proceeding along the right infraorbital rim circumferentially to the radix. On the left, the medially progressing incision tracked above the eyebrow along the superior orbital rim. An extending incision along the superior sternum connected the bilateral neck incisions. Doppler was then used to identify the left superficial temporal (ST) vasculature. After which, a coronal incision connected the superior points of the preauricular incisions, for later access to the cranial vault. All soft tissues superior to the orbits were not included in the allograft.

Beginning with the left neck dissection, the external jugular vein was identified, ligated, and divided. The platysma was divided, and the sternocleidomastoid was retracted, to allow for access and identification of the carotid sheath structures. The internal jugular vein was identified and followed to the facial vein, which was tagged and preserved with great care. Attention was turned to the arterial system, where the common carotid artery was circumferentially dissected and followed superiorly past the carotid bifurcation. The superior thyroid and ascending pharyngeal, occipital, and lingual arteries were tagged for later ligation, leaving the facial artery intact as the allograft pedicle. Attention was turned to the submandibular region, where the digastric muscle was divided and reflected laterally. The vasculature to the submandibular gland was ligated, and the gland was then dissected off the facial artery and allograft. The hypoglossal nerve was harvested for use as a potential nerve graft in the recipient operation.

Proceeding to the preauricular incision, the soft tissue of the left face was retracted medially. Using the

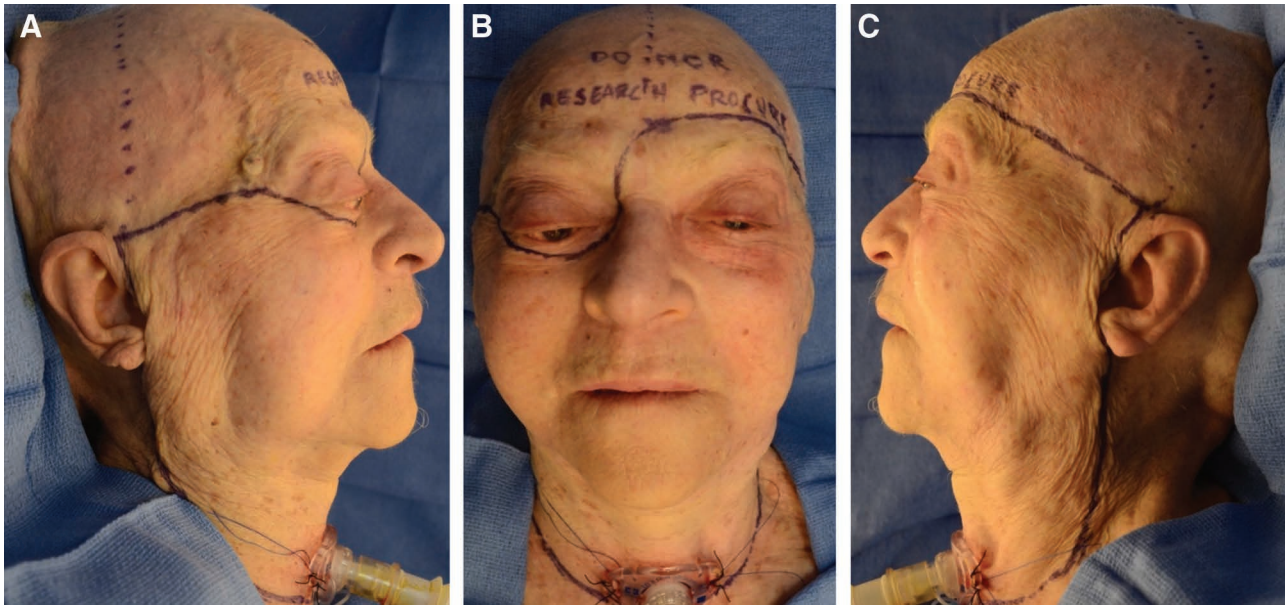

Fig. 1. Preoperative markings. A, Left lateral view (ie, right face). B, Anterior view. C, Right lateral view (ie, left face). Printed with permission and copyrights retained by Eduardo D. Rodriguez, MD, DDS.

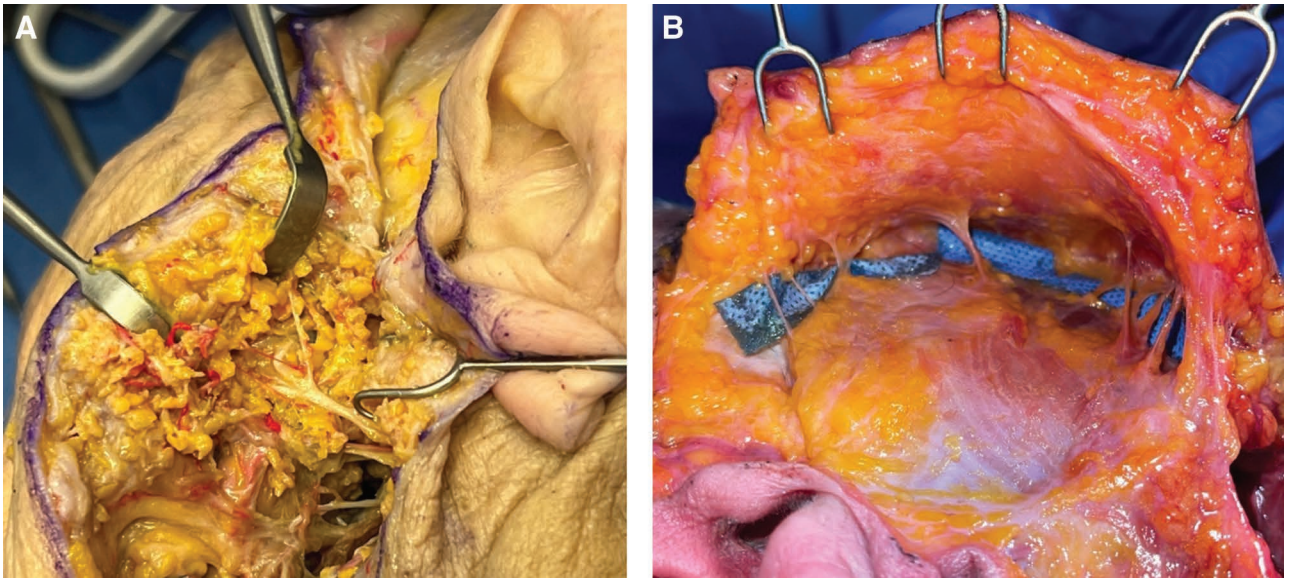

Fig. 2. Bilateral identification of the facial nerve. Identification of left facial nerve at the trunk using tragal pointer as a landmark (A). Identification of distal branches of the right facial nerve at their exit from the anterior parotid (B). Images from cadaveric dissection. Printed with permission and copyrights retained by Eduardo D. Rodriguez, MD, DDS.

tragal pointer as a landmark, the trunk of the facial nerve was identified, tagged, and clipped (Fig. 2). Proceeding superomedially and undermining a portion of the coronal flap, the ST vasculature was identified, having been previously approximated using Doppler. The ST vessels were dissected off the coronal flap down to the level of the zygomatic arch. While preserving the facial nerve, the dissection continued medially, remaining superficial to the masseter and halting at the anterior border of the parotid. Continuing inferiorly, the ST vasculature was isolated in continuity with the allograft.

Attention was then moved to the apex of the cranium, where the scalp dissection proceeded inferiorly in the subperiosteal plane bilaterally, until reaching the subsuperficial temporal fascia laterally and the superior orbital rim and radix medially. Care was taken to preserve the periorbital retaining ligaments on the left. On the right, the dissection was carried inferiorly along the nasomaxillary buttress lateral to the nasal bone. Bilateral zygomaticofrontal processes and zygomatic arches were exposed subperiosteally, preserving the attachments on the anterior zygoma.

Attending to the right side of the allograft, the neck dissection was carried out in a fashion analogous to the technique described above. The dissection then proceeded medially from the right preauricular incision, remaining superficial to the parotid fascia until reaching the anterior border of the parotid. There, the zygomatic, buccal, and marginal mandibular branches of the facial nerve were identified at their exit point from the parotid (Fig. 2). The nerves were then dissected retrograde before being tagged and divided, preserving maximum length.

A circumferential intra-oral incision was then made along the gingivobuccal mucosal junction, leaving a small cuff of mucosa on the maxilla and mandible. Bilateral exposure of the maxilla in the subperiosteal plane allowed the identification of the infraorbital nerves. On the left, the dissection proceeded laterally to approximately the mid zygoma, halting superior to the teeth roots. On the right, the dissection proceeded superiorly to expose the entire anterior maxilla and was connected with the descending dissection along the nasomaxillary buttress.

Turning to the mandibular component of the intra-oral incision, the dissection was carried inferiorly in the subperiosteal plane. Bilateral mental nerves were identified and tagged to be taken with the allograft. Ligamentous attachments at the mandibular symphysis were preserved. The dissection returned to the neck where the infrahyoid strap muscles were identified and a cuff of mylohyoid was taken with the allograft to be approximated during inset to avoid a salivary leak.

Osteotomies

Prefabricated cutting guides were then approximated to the bony landmarks, where contour engagement, in particular at the radix, right superomedial orbital rim, and left zygoma, served to confirm proper alignment. Screw fixation of the cutting guides was performed. To improve accuracy during inset, a reference drill point was made in the inferolateral component of the left orbitonasal box osteotomy. This reference point would be aligned with an analog point in the recipient, to allow for confirmation of alignment tactilely during inset, thereby minimizing disruption of soft-tissue and ligamentous attachments. Osteotomies were conducted beginning with the bilateral zygoma, followed by the orbitonasal box osteotomy, and the genial segment (Fig. 3). Positioning of these three osteotomies was selected to include necessary

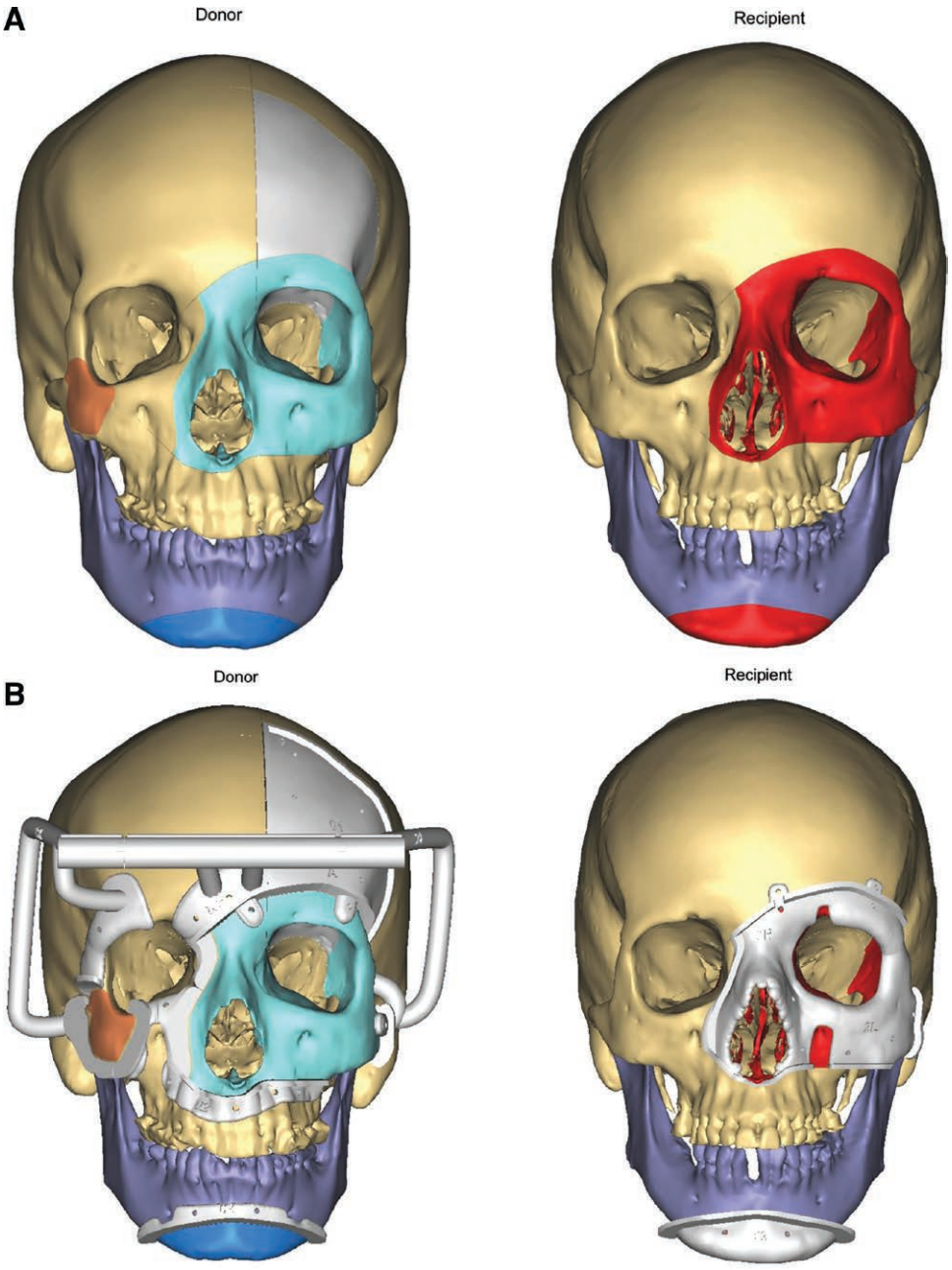

Fig. 3. Planned osteotomies, with liberated bony subunits are identified by color. Red colored components will be removed as part of the donor preparation, and Gray indicates the craniectomy, which will not be included in the transplant. Light blue, dark blue, and orange bony subunits are included in the allograft. Images are rendered with (top) and without (bottom) cutting guide placement for both the donor (A) and recipient operations (B). Printed with permission and copyrights retained by Eduardo D. Rodriguez, MD, DDS.

central facial functional units and to maintain ligamentous attachments of facial soft tissue for improved aesthetic outcomes. Adequate superior placement of the inferior maxillary osteotomy served to avoid damage to the teeth roots, which proved particularly challenging in edentulous donors. All osteotomy guides were fabricated using rapid prototyping technology to render the virtual models in polymethylmethacrylate.

Craniectomy, Intracranial, and Ocular Dissection

After the osteotomies, the cutting guides were removed. Leaving the liberated bony subunits in place, a craniectomy cutting guide was placed over the left frontal bone. After rigid fixation of the guide, a bioimpedance drill was used to perform the craniectomy, after which the dura was carefully freed, and the cranial and frontal bone segment was removed. The brain was retracted, and the

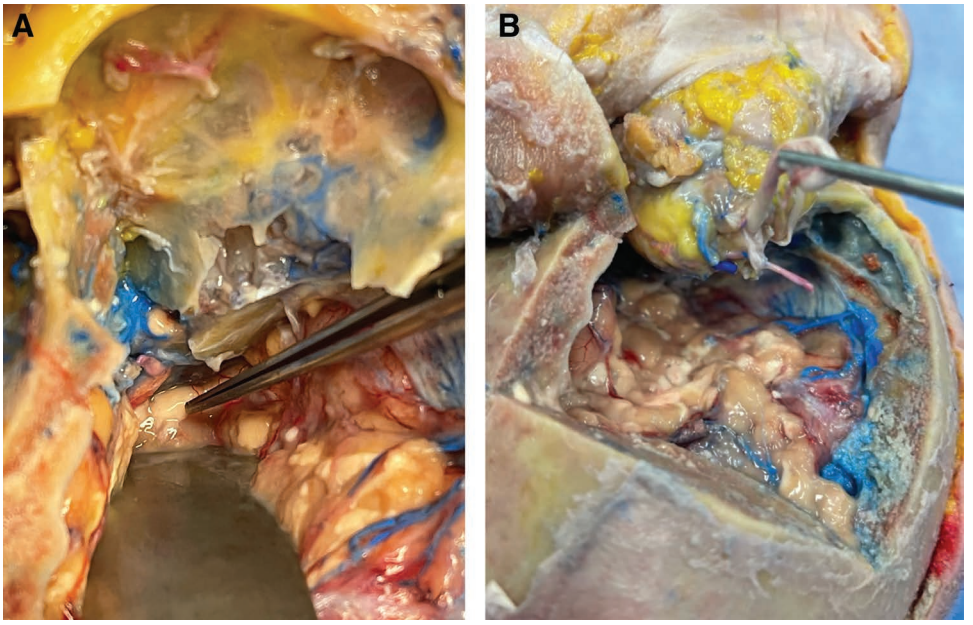

Fig. 4. Superior view of the optic nerve after craniectomy in a cadaveric donor. Before transection, with retraction of the brain, the optic nerve (indicated by forceps) is visible immediately distal to the optic chiasm (A). After release, the optic nerve is seen alongside the ophthalmic vasculature posterior to the annulus of Zinn (B). Red silicon injection indicates arterial system and blue indicated venous. Printed with permission and copyrights retained by Eduardo D. Rodriguez, MD, DDS.

superior orbital wall was carefully removed with a saw and Rongeur. The periorbital tissue was degloved, and anterior and posterior ethmoid vessels were identified and ligated. The optic nerve was identified within the optic foramen, and the bony component was unroofed to improve visualization. Proceeding proximal from the annulus of Zinn, the intracranial optic nerve was divided as near as possible to the chiasm, preserving maximal length (Fig. 4).

The vasculature posterior to the annulus of Zinn was visualized under the operating microscope. [**See Video 1 (online)**, which shows the microsurgical dissection of the posterior orbital structures.] After separation from the internal carotid system, continued bleeding from the periorbital structures was noted. After identification of the ophthalmic vessels and liberation of the optic nerve, the ipsilateral ST vessels were approximated, and appropriate vessel caliber and length were confirmed. Anastomoses were not performed, because this allowed indocyanine green (ICG) angiography in the external carotid system, to assess the degree of collateral perfusion to orbital and periorbital structures. [**See Video 2 (online)**, which shows the evaluation of full allograft, periorbital, and orbital structure perfusion using ICG.] Following this, the facial allograft was re-inset per the donor family's wishes, and incisions were closed.

Recipient Preparation

While the operative procedure described above was performed on a brain-dead donor, recipient preparation and allograft inset were unable to be performed given the single patient. Therefore, the following techniques are described based on the OR cadaveric rehearsals.

With the exception of the cranial incision, skin and soft tissue markings described above were replicated in the recipient. Neck dissections were then conducted in a fashion similar to the donor while minimizing soft tissue undermining and preserving critical structures. Facial exposure was conducted through bilateral preauricular incisions, while the genial portion was accessed inferiorly. The facial nerve was identified at the distal branches on the right and at the trunk on the left. The dissection remained largely superficial to the mimetic musculature, save for the subperiosteal undermining necessary for cutting guide placement. Osteotomies were similar to the donor; however, the rightmost component of the orbitonasal box osteotomy was maintained as medially as possible to avoid violation of the right maxillary sinus and lacrimal outflow tract (Fig. 3). No craniectomy was performed. After osteotomies, attention was turned to the remaining intraorbital and intranasal contents, where volume was preemptively reduced to account for postoperative edema. Remnant intact ocular muscles, as well as the stump of the optic nerve and any remaining intraorbital vasculature, were identified, tagged, and preserved.

Allograft Inset

The allograft was overlayed onto the recipient, and points of bony contact were assessed and burred as needed to smooth remnant edges and improve inset accuracy. Rigid fixation of the genial component was conducted first, followed by the right anterior zygoma, and then the orbitonasal box osteotomy. When inset in a living donor, left external carotid anastomosis would immediately follow genial fixation, to limit orbital ischemia time. Fixation was achieved using bicortical

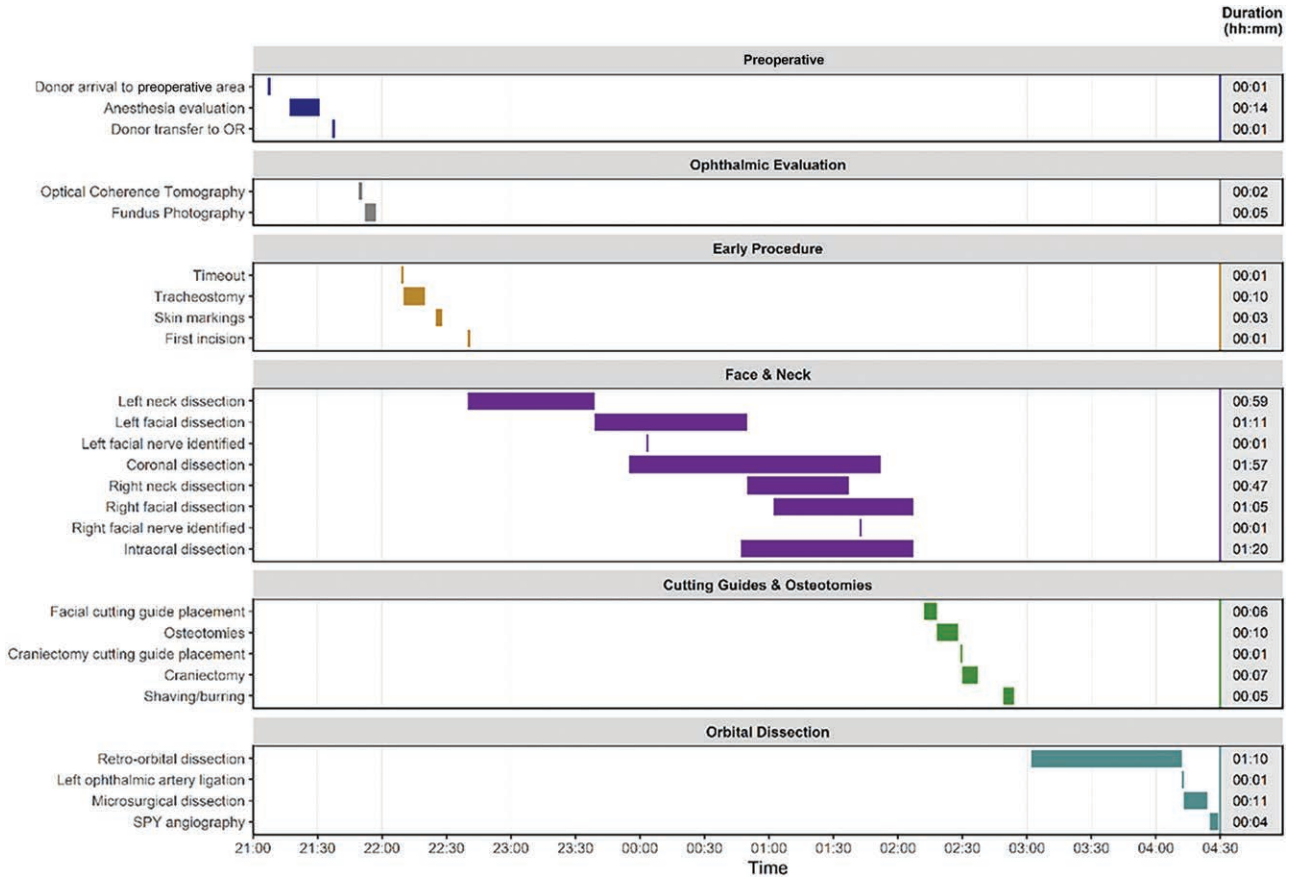

Fig. 5. Timeline of events during RP, including concomitant events and duration in hours and minutes. Printed with permission and copyrights retained by Eduardo D. Rodriguez, MD, DDS.

positional lag screws and completed with miniplates; however, the right zygomatic component was inset using only screws. For the box osteotomy, the optic nerve was coapted, followed by plating of the medial maxillary component. Before plating the left lateral zygomaticomaxillary component, alignment was confirmed using the pre-drilled reference points (Fig. 3). Great care was taken to avoid damaging the ophthalmic-to-ST anastomosis, leaving appropriate space, thereby avoiding compression from postoperative edema. Finally, plating of the superior (frontal bone) and inferior (maxillary) components of the box osteotomy was completed.

After rigid fixation, the facial nerves were coapted as distally as possible on the right (to reduce the risk of postoperative synkinesis), and at the level of the trunk on the left. The intra-oral incision was closed in a circumoral fashion at the gingivobuccal junction. The skin envelope was then draped over the recipient, excess skin was trimmed, and incisions were closed.

RESULTS

Timing

The timing of major events in the RP is outlined in Figure 5. The procurement took approximately 7 hours and 22 minutes, starting from donor arrival to the preoperative area and ending with completion of ICG angiography. Time from ophthalmic artery transection to beginning ophthalmic-ST anastomosis was 12 minutes.

Vascular and Ocular Considerations

Ophthalmic vessels were safely identified in all OR CRs, as well as the RP. Appropriate pedicle length was seen in all cases, as measured by tensionless apposition with the ST artery and vein, and vessel caliber was uniformly appropriate. Maximal ophthalmic pedicle length was greater than 2.5 cm. In all cases, the optic nerve was coapted or opposed without tension.

Inset

Examining preoperative anthropometric differences among cadavers, Student *t* tests comparing the mean donor and recipient measurements demonstrated no significant differences (Table 2). Overall, osteotomy inset accuracy by subunit demonstrated marginal improvement throughout rehearsals. Inset of all subunits was highly accurate, as evidenced by often 0.5- to 1.5-mm median absolute difference between actual and projected outcomes (Fig. 6). Pearson correlation coefficients assessed the relationship between preoperative anthropometric donor-recipient differences and postoperative inset accuracy by bony subunit. This demonstrated that greater donor-recipient mismatch in orbital and upper facial heights had the greatest

Table 2. Comparison of Mean Preoperative Donor and Recipient Bony Measurements

	Donor		Recipient		
	Mean	SD	Mean	SD	*P*
Biparietal distance (mm)	138.30	3.54	139.42	1.70	0.52
Fronto-occipital distance (mm)	182.50	4.53	184.08	7.30	0.71
Bizygomatic distance (mm)	88.80	8.06	94.22	7.47	0.18
Bigonial distance (mm)	91.53	6.47	96.52	4.72	0.32
Medial intercanthal distance (mm)	21.13	3.81	21.13	4.16	0.95
Lateral intercanthal distance (mm)	94.28	4.17	98.38	2.35	0.08
Left orbital width (mm)	36.62	2.27	38.05	2.17	0.20
Left orbital height (mm)	35.25	2.40	34.27	1.98	0.52
Right orbital width (mm)	36.80	2.94	38.77	1.60	0.16
Right orbital height (mm)	35.28	2.18	34.63	1.98	1.00
Upper facial height (mm)	56.67	4.98	57.30	2.94	0.61
Lower facial height (mm)	63.98	5.32	65.30	1.42	0.80
SNA (degrees)	85.65	5.23	86.18	4.54	0.75
SNB (degrees)	81.32	5.09	79.78	7.22	0.80
Mandibular Angle (degrees)	123.15	7.67	129.25	7.47	0.38

No statistically significant differences were found. Printed with permission and copyrights retained by Eduardo D. Rodriguez, MD, DDS.

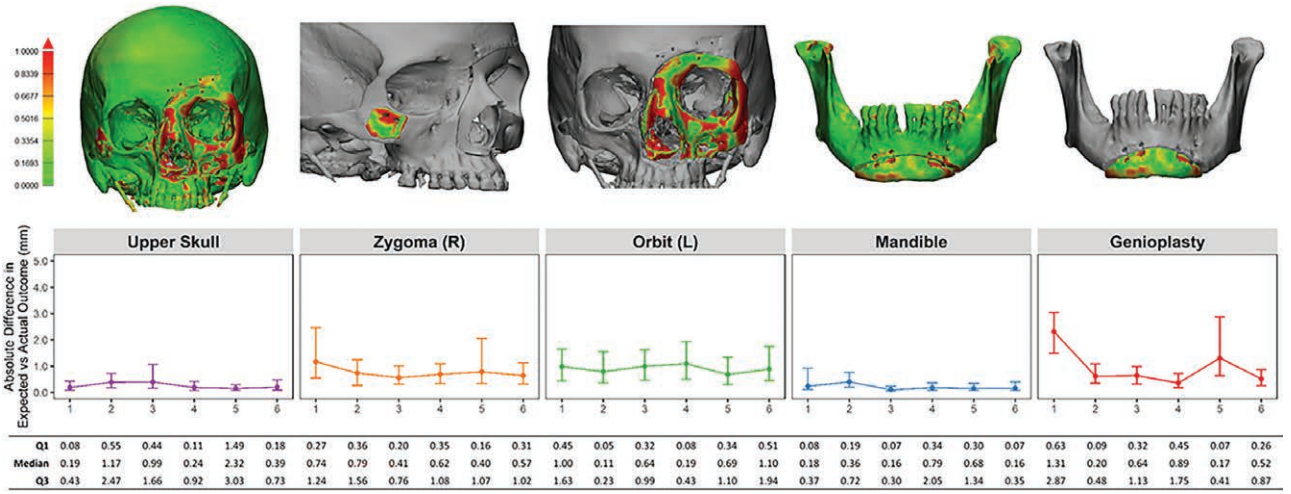

Fig. 6. Expected vs actual osteotomy inset outcomes by subunit. Heatmap of inset accuracy by subunit (top row). Median and interquartile range for absolute difference in millimeters (line graph and table). Measured by comparing postoperative CT scans with the projected outcome based on virtual surgical planning. Printed with permission and copyrights retained by Eduardo D. Rodriguez, MD, DDS.

Table 3. Pearson Correlation Coefficients Assessing the Relationship between Preoperative Anthropometric Donor-Recipient Differences and Postoperative Inset Accuracy by Bony Subunit

	Bizygomatic	Medial Intracantal	Lateral Intracantal	Left Orbital Width	Left Orbital Height	Upper Facial	Lower Facial	SNA	SNB	Mandibular Angle
Left orbital box osteotomy	-0.27*	-0.33	-0.18*	-0.13*	0.85*	0.72*		-0.39*		
Genioplasty							0.46		-0.01	-0.41*
Right zygoma	-0.27		0.45			0.47				

*Statistically significant correlation. Printed with permission and copyrights retained by Eduardo D. Rodriguez, MD, DDS.

correlation with postoperative inset inaccuracy of the orbitonasal box osteotomy (Table 3).

DISCUSSION

Cadaveric rehearsals improve the accuracy of allograft inset and reduce ischemia time for FT procedures, both of which are believed to improve aesthetic outcomes and reduce postoperative complications.[10,13,14] These benefits are achieved by enabling clinicians to plan the optimal operative approach, practice techniques, prepare necessary specialized staff and equipment, improve communication, and identify potential danger points for which the risk of error is high. In light of these benefits in FT, the necessity of these rehearsals in preparation for

complex and novel procedures—such as FWET—cannot be understated.

Few surgeons have considered whole eye transplantation, owing to the poor regenerative capacity of the central nervous system, of which the optic nerve and retinal ganglion cells are a direct extension. However, recent advancements in immunobiology have led clinicians to reconsider this orthodoxy.[15] Irrespective of vision restoration, transplantation of the globe as an organic prosthetic holds the promise to improve aesthetic outcomes and mitigate complications of enucleation and ocular prosthetics. Further, in light of the immune privileged nature of the orbit, its inclusion in a facial allograft portends only a limitedly increased rejection burden.[16]Thus, in light of its potential benefits and limited increased risk, multiple cadaveric models exploring surgical approaches to FWET have been published.[9,17–20]

Through preparation for potential in vivo FWET, this study formalizes an approach feasible for clinical translation. As rehearsals followed identification of a potential recipient, the limitations posed by a real clinical context required technical adaptation. In particular, the lack of patent ophthalmic vessel remnants precluded anastomosis to the potential recipient's native vasculature. Although external carotid collateral flow to the orbit has been demonstrated in previous studies and affirmed in our ICG angiography, it serves only to abate short-term ischemia and is not sufficient for long-term viability.[21] Thus, to address this, we opted for an ophthalmic-to-ST anastomosis as first proposed in FWET by Davidson et al.[19] Since their proposal, ophthalmic artery length and appropriate vessel caliber has been confirmed on anatomic studies.[22,23] Further, although previous studies suggested the necessity for vein grafting, by including the intracranial ophthalmic segment and releasing the annulus of Zinn, we achieved the appropriate length for tensionless anastomoses without vein grafting.

Although this approach was undertaken due to clinical constraints, the ophthalmic-to-ST anastomosis provided the added benefit of considerably reducing retinal ischemia time. Abbas et al found that while retinal ganglion cells could survive relatively prolonged ischemia, bipolar cells within the retina, which are integral to the maintenance of sight, would begin to fail after approximately 20 minutes, with complete irreparable loss at 45 minutes.[24] Thus, by opting for the ophthalmic-to-ST approach outlined above, we limit retinal ischemia time before release of the allograft in the donor. Further, following inset in the recipient, this approach allows a single anastomosis of the external carotid to perfuse both the face and globe.

CONCLUSIONS

We present the most extensive cadaveric rehearsal study assessing the feasibility of concomitant FWET to date. Through preparation for potential in vivo FWET, this study formalizes an approach feasible for clinical translation. Although restoration of vision likely remains out of reach, globe survival is possible. In judiciously selected patients, FWET may offer improved aesthetic outcomes while avoiding complications of enucleation and orbital prosthetics.

Eduardo D. Rodriguez, MD, DDS
Hansjorg Wyss Department of Plastic Surgery at NYU
Grossman School of Medicine
222 East 41st Street, 6*th* floor
New York, NY 10017
E-mail: eduardo.rodriguez@nyumc.org

DISCLOSURES

Eduardo D. Rodriguez has received speaker Honoria from DePuy Synthes for work unrelated to this study. All the other authors have no financial interest to declare in relation to the content of this article. This study was funded by the Reconstructive Transplantation Research Award (W81XWH-15-2-0036) from the Department of Defense, with institutional support from New York University Langone Health.

PATIENT CONSENT

The patient provided written consent for the use of his image.

REFERENCES

1. Parker A, Chaya BF, Rodriguez-Colon R, et al. Recipient selection criteria for facial transplantation: a systematic review. *Ann Plast Surg.* 2022;89:105–112.
2. Diep GK, Berman ZP, Alfonso AR, et al. The 2020 facial transplantation update: a 15-year compendium. *Plast Reconstr Surg Glob Open.* 2021;9:e3586.
3. Greenfield JA, Kantar RS, Rifkin WJ, et al. Ocular considerations in face transplantation: report of 2 cases and review of the literature. *Ophthal Plast Reconstr Surg.* 2019;35:218–226.
4. Shokri T, Saadi R, Wang W, et al. Facial transplantation: complications, outcomes, and long-term management strategies. *Semin Plast Surg.* 2020;34:245–253.
5. Sosin M, Mundinger GS, Dorafshar AH, et al. Eyelid transplantation: lessons from a total face transplant and the importance of blink. *Plast Reconstr Surg.* 2015;135:167e–175e.
6. Bramstedt KA, Plock JA. Looking the world in the face: the benefits and challenges of facial transplantation for blind patients. *Prog Transplant.* 2017;27:79–83.
7. Sami D, Young S, Petersen R. Perspective on orbital enucleation implants. *Surv Ophthalmol.* 2007;52:244–265.
8. Bonaque-González S, Amigó A, Rodríguez-Luna C. Recommendations for post-adaption care of an ocular prosthesis: a review. *Cont Lens Anterior Eye.* 2015;38:397–401.
9. Laspro M, Chaya BF, Brydges HT, et al. Technical feasibility of whole-eye vascular composite allotransplantation: a systematic review. *Plast Reconstr Surg Global Open.* 2023;11:e4946.
10. Ramly EP, Alfonso AR, Berman ZP, et al. The first successful combined full face and bilateral hand transplant. *Plast Reconstr Surg.* 2022;150:414–428.
11. Pomahac B, Pribaz J, Eriksson E, et al. Three patients with full facial transplantation. *N Engl J Med.* 2012;366:715–722.
12. Kauke M, Panayi AC, Tchiloemba B, et al. Face Transplantation in a black patient—racial considerations and early outcomes. *N Engl J Med.* 2021;384:1075–1076.
13. Sosin M, Ceradini DJ, Hazen A, et al. Total face, eyelids, ears, scalp, and skeletal subunit transplant cadaver simulation: the culmination of aesthetic, craniofacial, and microsurgery principles. *Plast Reconstr Surg.* 2016;137:1569–1581.

14. Brown EN, Dorafshar AH, Bojovic B, et al. Total face, double jaw, and tongue transplant simulation: a cadaveric study using computer-assisted techniques. *Plast Reconstr Surg.* 2012;130:815–823.
15. Bourne D, Li Y, Komatsu C, et al. Whole-eye transplantation: a look into the past and vision for the future. *Eye (Lond).* 2017;31:179–184.
16. Zor F, Karagoz H, Kapucu H, et al. Immunological considerations and concerns as pertinent to whole eye transplantation. *Curr Opin Organ Transplant.* 2019;24:726–732.
17. Siemionow M, Bozkurt M, Zor F, et al. A new composite eyeball-periorbital transplantation model in humans: an anatomical study in preparation for eyeball transplantation. *Plast Reconstr Surg.* 2018;141:1011–1018.
18. Bravo MG, Granoff MD, Johnson AR, et al. Development of a new large-animal model for composite face and whole-eye transplantation: a novel application for anatomical mapping using indocyanine green and liquid latex. *Plast Reconstr Surg.* 2020;145:67e–75e.
19. Davidson EH, Wang EW, Yu JY, et al. Total human eye allotransplantation: developing surgical protocols for donor and recipient procedures. *Plast Reconstr Surg.* 2016;138:1297–1308.
20. Siemionow M, Bozkurt M, Zor F, et al. Reply: a new composite eyeball-periorbital transplantation model in humans: an anatomical study in preparation for eyeball transplantation. *Plast Reconstr Surg.* 2019;143:439e–440e.
21. Chen SN, Huang J, Hwang JF. Bilateral retinal artery occlusions with carotid artery occlusions-ocular and cerebral hemodynamic changes. *Am J Ophthalmol Case Rep.* 2020;20:100959.
22. Rubio RR, Gandhi S, Vigo V, et al. An anatomic feasibility study for revascularization of the ophthalmic artery, Part I: intracanalicular segment. *World Neurosurg.* 2020;133:e893–e901.
23. Rubio RR, Vigo V, Gandhi S, et al. An anatomical feasibility study for revascularization of the ophthalmic artery. Part II: intraorbital segment. *World Neurosurg.* 2020;133:401–408.
24. Abbas F, Becker S, Jones BW, et al. Revival of light signalling in the postmortem mouse and human retina. *Nature.* 2022;606:351–357.